

## Deep low-frequency earthquakes in tectonic tremor along the Alaska-Aleutian subduction zone

Justin R. Brown,<sup>1</sup> Stephanie G. Prejean,<sup>2</sup> Gregory C. Beroza,<sup>1</sup> Joan S. Gomberg,<sup>3</sup> and Peter J. Haeussler<sup>2</sup>

Received 18 May 2012; revised 30 October 2012; accepted 13 November 2012; Published 26 March 2013.

[1] We characterize and locate tremor not associated with volcanoes along the Alaska-Aleutian subduction zone using continuous seismic data recorded by the Alaska Volcano Observatory and the Alaska Earthquake Information Center from 2005 to present. Visual inspection of waveform spectra and time series reveal dozens of 10 to 20 min bursts of tremor along the length of the Alaska-Aleutian subduction zone. We use autocorrelation to demonstrate that these tremor signals are composed of hundreds of repeating low-frequency earthquakes (LFEs). The tremor activity we characterize is localized in four segments, from east to west: Kodiak Island, Shumagin Gap, Unalaska, and Andreanof Islands. Although the geometry, age, thermal structure, frictional, and other relevant properties of the Alaska-Aleutian subduction zone are poorly known, these characteristics are likely to differ systematically from east to west. Locations near Kodiak Island are the most reliable because station coverage is more complete. LFE hypocenters in this region are located on the plate interface near the down-dip limit of the 1964  $M_w$  9.2 Alaska earthquake rupture area. LFE hypocenters in the remaining areas along the arc are also located down-dip of the most recent  $M_w$  8+ megathrust earthquakes. Although these locations are less well constrained, our results support the hypothesis that tremor activity marks the down-dip rupture limit for great megathrust earthquakes in this subduction zone. Lastly, there is no correlation between the presence of tremor and particular aspects of over-riding or subducting plate geology or coupling. It appears that LFEs are a fundamental characteristic of the Alaska-Aleutian subduction zone.

**Citation:** Brown, J. R., S. G. Prejean, G. C. Beroza, J. S. Gomberg, and P. J. Haeussler (2013), Deep low-frequency earthquakes in tectonic tremor along the Alaska-Aleutian subduction zone, *J. Geophys. Res. Solid Earth*, 118, 1079–1090, doi:10.1029/2012JB009459.

### 1. Introduction

[2] The Alaska-Aleutian subduction zone forms the plate boundary between the Pacific and North American plates for 3800 km between eastern Russia and central Alaska [Ruppert *et al.*, 2007]. From east to west: the sense of plate motion ranges from trench normal to transform, the velocity of relative plate motion ranges from about 5.1 to 7.5 cm/yr [DeMets *et al.*, 1994], and the Pacific Plate ranges in age from ~35 to ~63 Ma (Figure 1).

[3] The Alaska-Aleutian subduction zone is both seismically and volcanically very active. This margin ruptured in

four  $M_w$  8+ earthquakes within the last 75 yr: 1938  $M_w$  8.2 Shumagin Islands, 1957  $M_w$  8.6 Andreanof Islands, 1964  $M_w$  9.2 Good Friday, and 1965  $M_w$  8.7 Rat Islands (Figure 1). While some portions are clearly locked between large earthquakes and accommodate the majority of deformation seismically, other areas, such as the Shumagin Gap, appear to lack large earthquakes and may deform aseismically [Hauksson *et al.*, 1984; Freymueller *et al.*, 2008]. Tremor and slow slip, commonly referred to as “episodic tremor and slip”, occur in other circum-Pacific subduction zones and in other parts of plate interfaces that are transitional between seismic and aseismic slip. Ohta *et al.* [2006] identified slow slip/creep events in the south-central Alaska portion of the subduction zone to the east of our study area, and Peterson *et al.* [2011] also identified tremor-like signals along the Alaska-Aleutian subduction zone.

[4] Tremor is intrinsically difficult to study due to its low signal-to-noise ratio (snr). Studying nonvolcanic tremor in the Alaska-Aleutian subduction zone is particularly challenging for three reasons: (1) Harsh weather conditions in this sparsely populated part of the world generate strong seismic noise. (2) Seismic and geodetic studies are restricted to land-based linear instrument deployments westward of

All supporting information may be found in the online version of this article.

<sup>1</sup>Department of Geophysics, Stanford University, Stanford, California, USA.

<sup>2</sup>U.S. Geological Survey, Alaska Science Center, Anchorage, Alaska, USA.

<sup>3</sup>U.S. Geological Survey, University of Washington, Department of Earth and Space Sciences, Seattle, Washington, USA.

Corresponding author: J. R. Brown, Department of Geophysics, Stanford University, 397 Panama Mall, Stanford, CA 94305-2215, USA. (jrbrown5@stanford.edu)

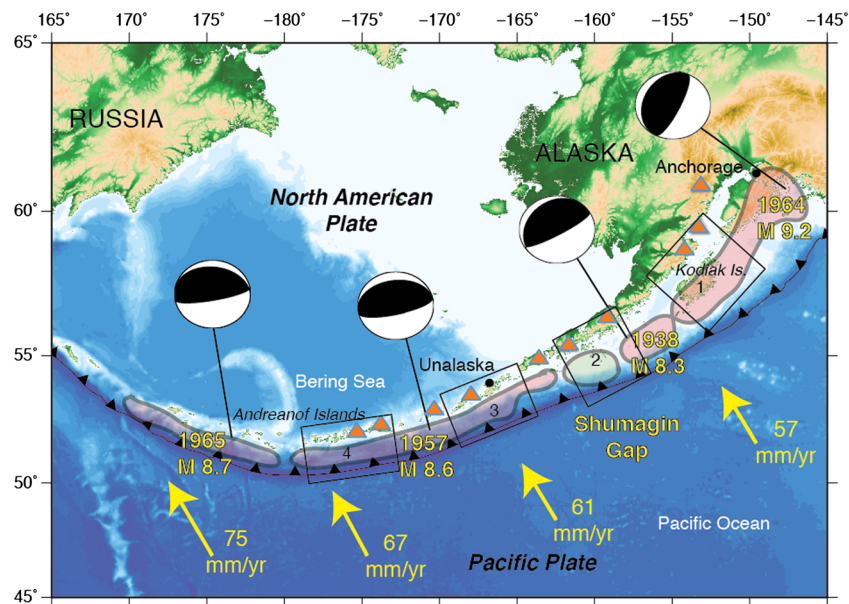


**Figure 1.** Regional bathymetric/topographic map of the Alaska-Aleutian Subduction Zone. Triangle-lined line denotes subduction megathrust. Yellow arrows indicate the motion of the subducting Pacific Plate relative to the North American Plate. Rupture areas for the four largest megathrust events in the 20th century are shaded in pink and are shown with their respective focal mechanisms. Volcanoes with elevated activity during 2005–2010 are shown as orange triangles. Numbered boxes 1 through 4 correspond to the Kodiak island, Shumagin Gap, Unalaska, and Andreanof Islands regions where tremor is characterized in this study, respectively.

Kodiak Island due to the expense and logistics of amphibious geophysical studies. (3) The Alaska-Aleutian Arc seismic records include frequent signals from volcanoes, earthquakes, and possibly hydrothermal activity related to magmatic activity.

[5] Deep, nonvolcanic tremor was first discovered in southwest Japan [Obara, 2002] and in Cascadia it was found to occur during episodes of slow slip [Rogers and Dragert, 2003]. Our understanding of tremor is evolving rapidly and accounts of the state of knowledge can be found in several review papers [Schwartz and Rokosky, 2007; Gomberg, 2010; Rubinstein et al., 2010; Beroza and Ide, 2011]. In this paper we focus on the analysis of low-frequency earthquakes (LFEs) as a way of understanding tremor. Brown et al. [2009] demonstrated that low-frequency earthquakes comprise tremor on the plate interface down-dip of the locked portion of three subduction zones. LFEs are small earthquakes (less than magnitude  $\sim 2$ ) with amplitudes that decay at higher frequencies, particularly above  $\sim 10$  Hz that occur during episodes of deep tremor in southwest Japan [Katsumata and Kamaya, 2003; Shelly et al., 2006] and belong to a newly discovered class of slow earthquakes [Ide et al., 2007]. Tremor generation may be related to fluid release during oceanic slab dehydration [Katsumata and Kamaya, 2003]; however, empirical moment tensor analysis reveals that LFEs are generated by shear slip [Ide et al., 2007] on the deep extension of the plate boundary [Shelly et al., 2007a]. The spectral characteristics of tremor and LFEs are essentially identical [Shelly et al., 2006] and comparison of tremor and LFE waveforms indicate that tremor in southwest Japan is comprised of LFE swarms [Shelly et al., 2006; Shelly et al., 2007b; Brown et al., 2008].

[6] Although tremor was detected along the Alaska-Aleutian Arc [Peterson et al., 2011], not much is known about its location and possible relationship to slip in large earthquakes.

[7] For this paper, we scan nonvolcanic tremor-like signals previously cataloged by the Alaska Volcano Observatory (AVO) recorded throughout the Alaska-Aleutian subduction zone using running autocorrelation to detect LFEs within tremor [Brown et al., 2008] and to distinguish deep tremor from other signals (long-period events, volcanic tremor, and noise). Once we detect LFEs within tremor, we relocate them using a combination of waveform-based differential arrival time measurements and the double-difference location technique [Waldhauser and Ellsworth, 2000]. We find that tremor appears to occur on the down-dip extension of the locked portion of the plate interface, and that it occurs in a wider range of subduction zone environments than had previously been recognized. An apparent depth dependence from east to west along the arc suggests that temperature may play a controlling role in tremor occurrence, but other more complex factors could influence its occurrence as well.

## 2. Tectonic Tremor Versus Volcanic Tremor

[8] Volcanic tremor is a long duration low-amplitude signal that, in most cases, occurs within the upper 5 km of the crust within a volcanic edifice [McNutt, 1992]. Volcanic tremor can be attributed to a wide variety of processes including fluid migration and degassing, and is commonly associated with eruptive activity [e.g., Chouet, 1985; Julian, 1994; Hellweg, 2000; Johnson and Lees, 2000]. Discriminating between nonvolcanic, or what we refer to as “tectonic

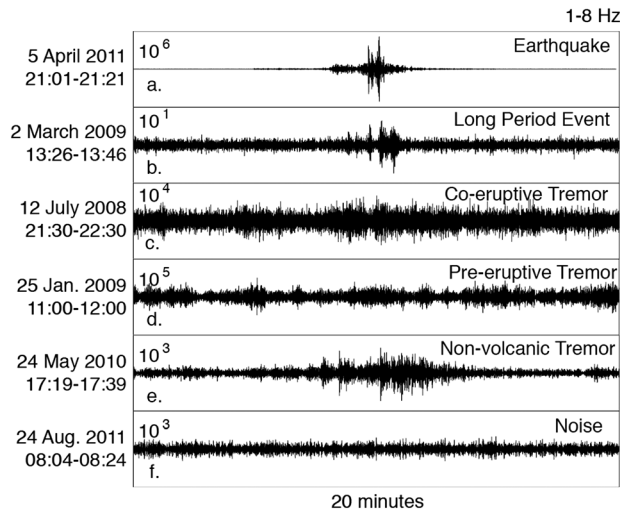


**Figure 2.** Examples of (a) an earthquake, (b) deep long period from 18 km depth, (c) co-eruptive tremor at Okmok Volcano, (d) pre-eruptive tremor at Redoubt Volcano, (e) nonvolcanic tremor in the Eastern Aleutians, and (f) noise in the Aleutians. Amplitudes are in nm/s.

tremor” from here onwards, and volcanic tremor in the Alaska-Aleutian subduction zone can be challenging due to similarities in their characteristics and low snr. All of the seismic instrumentation in the Aleutians is deployed on volcanic islands, and many of the volcanoes are active.

[9] It should be possible to discriminate between volcanic and tectonic tremor using their spectra. Tectonic tremor energy is confined to the 1–10 Hz band whereas volcanic tremor is often excited between 1–5 Hz and can extend to higher frequencies as well. In addition, tectonic tremor is inharmonic whereas volcanic tremor can be both harmonic and inharmonic. Because of the wide range of behavior for volcanic tremor, neither of these differences reliably discriminates one signal from the other. Depth and location, on the other hand, can be strongly diagnostic of volcanic versus tectonic tremor. Typically volcanic tremor originates at shallow depths ( $< 5$  km) [McNutt, 1992], whereas tectonic tremor in subduction zones locates at the deep extension of the locked portion of the megathrust [Brown et al., 2009] at depths of  $\sim 40$  km. In this paper, we use the locations of LFEs within tectonic tremor to show that the signal is tectonic in origin.

### 3. Methods

[10] Our approach to characterizing tremor sources involves: (1) identifying tremor-like signals, (2) detecting and timing LFEs within these signals, and (3) locating LFE sources. For the most part, the technique matches that of Brown et al. [2008].

#### 3.1. Identification of Tremor-Like Signals

[11] In order to study low-frequency earthquakes, we first identify the tremor-like signals where LFEs may occur. Tectonic tremor detection in subduction zones has been successfully automated in the Cascadia subduction zone [Kao et al., 2007; Kao et al., 2008; Wech and Creager,

2008]. Unfortunately, the recording geometry in the Alaska-Aleutian margin is limited by geography compared to other subduction settings where tremor has been observed and prevents the successful application of these approaches. For that reason, we use visual inspection to identify possible tremor episodes in this more observationally challenging environment.

[12] The U.S. Geological Survey AVO monitors seismic activity around volcanoes throughout the volcanic arc using a combination of short-period, high gain, and broadband sensors. An AVO seismologist inspects spectrograms of all operating channels every 12 h and logs seismic activity that may be generated by diverse mechanisms, including: volcanic tremor, volcano-tectonic earthquakes, long-period earthquakes, deep magmatic-related activity, cultural noise, weather, and tectonic tremor (Figure 2). We searched the AVO log for any reference to tremor-like activity from 2005 to present, and visually inspected waveform spectra during these periods using Swarm and the online monitoring tool Volcano Analysis and Visualization Environment [Cervelli et al., 2002].

[13] A signal is considered a tremor if it meets the following criterion from visual inspection of the waveforms and spectrograms. (1) The signal must be band-limited to 1–10 Hz to avoid analyzing high-frequency volcanic tremor, weather, and noise (Figure 3). (2) The waveforms should share a similar shape for at least five stations within a 50 km radius, but not beyond. We use this criterion to ensure a local source and exclude teleseisms. (3) The duration of the signal must be at least 5 min (Figure 4). For subduction environments where deep tectonic tremor signals originating on the plate interface are known to occur, these criteria hold true [Obara, 2002; Schwartz and Rokosky, 2007; Brown et al., 2009, Figures 3 and 4]. Table 1 lists the tremor-like signals analyzed in this study. We note that, due to the inconsistent visual inspection and the variability of noise levels, the tremor catalog is likely far from complete during 2005–2010. Rather this catalog represents the clearest recordings

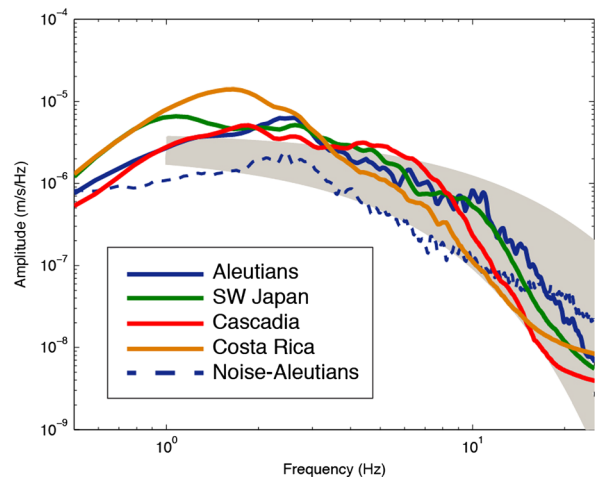


**Figure 3.** Velocity spectra of tectonic tremor from circum-Pacific subduction zones. The stacked noise spectrum from Unalaska is the blue dashed curve. The shaded gray area are the attenuation curves using  $\exp(-\pi ft/Q)$  for  $t = 19$  s and  $Q = 200$ –400.

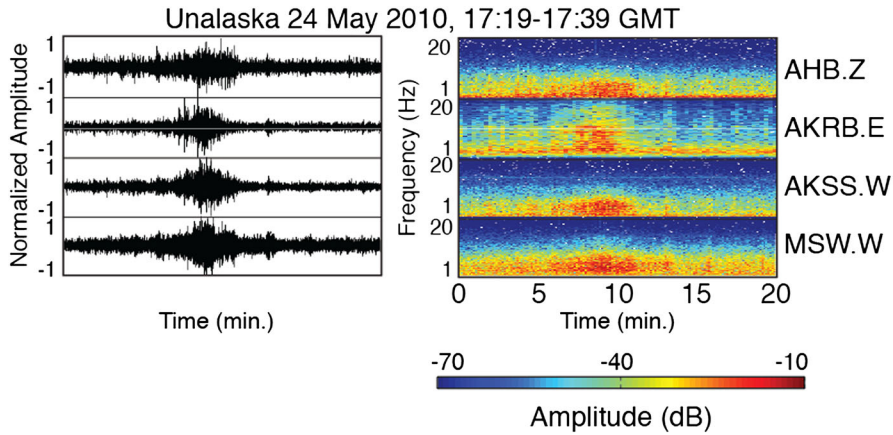


**Figure 4.** Tectonic tremor time series (left) and spectrograms (right) at four stations during the 24 May 2010 tremor episode in the Unalaska region. Time series are normalized. Spectrograms in all plots range from 1 to 20 Hz with spectral amplitudes in decibels.

of tectonic tremor along the Alaska-Aleutian Arc during that period.

### 3.2. Low-Frequency Earthquake Detection

[14] Once the tremor was identified we searched for repeating LFEs within the signal using the running autocorrelation method of *Brown et al.* [2008]. We analyzed continuous velocity seismograms recorded at a minimum of five stations for the time periods and locations listed in Table 1. Data were bandpass filtered from 1–8 Hz and autocorrelation was used to find waveforms that nearly repeat across the seismic network of interest. We use all available data that is sufficiently close to record a common signal. For example, we are blind to tremor in the central portion of the 1957 rupture zone (between boxes 3 and 4 in Figure 1) due to a large hole in seismic networks. As a result, the coverage is uneven along the arc. Detections and locations are more reliable for areas closest to mainland Alaska where station coverage is densest.

[15] We performed a first pass at running-window autocorrelation to search for similarity at all stations and over

all components. Forty minutes of continuous data were segmented into 8 s windows lagged by 0.5 s. The first half of the signal presumably includes no tremor whereas the last half of the 40 min includes the tremor-like signal identified in the AVO catalog (Figure 5). The 8 s windows are longer than the 6 s window length used previously by *Brown et al.* [2008], but we found it to be optimal for this study because moveout of the seismic phases were unknown across the network a priori, which may lead to greater variation in LFE depths.

[16] If we use shorter time windows the result yields fewer significant detections. This occurs because the stations furthest from the source have later phase arrivals than stations closest to the source. If the window only captures arrivals for stations closer to the source there will not be an arrival for stations further away and the corresponding window at those stations are correlating noise, which depresses the summed autocorrelation coefficient. Conversely, longer time windows also resulted in fewer significant detections, because they include nonsimilar parts of the waveform, which result in a lower snr. Longer time windows are not

**Table 1.** Catalog of Tremor Bursts Throughout the Alaska-Aleutian Subduction Zone

Year	Month	Day	Hour : Min	Location
2007	January	31	13:14	Kodiak Island
2007	April	7	7:14	Shumagin Gap
2007	May	8	23:50	Unalaska
2007	July	24	3:32	Andreanof Islands
2008	May	27	4:30	Kodiak Island
2008	July	13	19:54	Andreanof Islands
2008	September	26	10:10	Unalaska
2008	November	7	5:58	Unalaska
2008	November	7	6:46	Unalaska
2008	November	7	10:02	Unalaska
2008	December	10	16:05	Kodiak Island
2008	December	11	3:17	Kodiak Island
2008	December	11	3:30	Kodiak Island
2008	December	11	11:19	Kodiak Island
2009	February	22	0:57	Unalaska
2010	March	24	21:32	Shumagin Gap
2010	May	24	17:08	Unalaska
2010	May	24	17:25	Unalaska

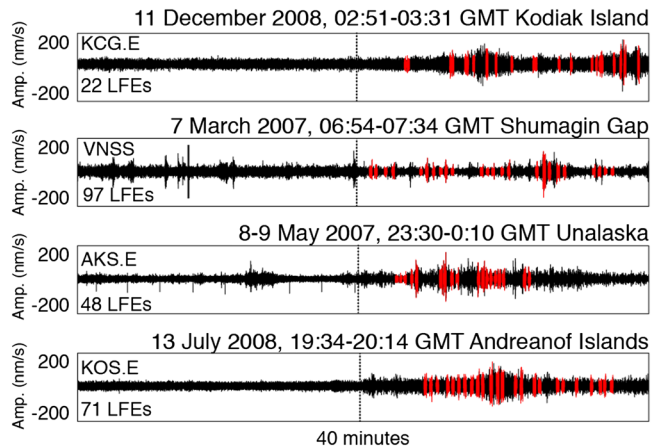


**Figure 5.** Detections (shown in red) of repeating LFEs within 40 min of continuous data from (a) Kodiak Island, (b) Shumagin Gap, (c) Unalaska, and (d) Andreanof Islands.

optimal because the autocorrelation process will be approximately twice as long for roughly the same number of windows if the successive lag is the same. We also experimented with different lags. The trade-off here is that computation time increases as the spacing decreases, but large lags yield fewer detections because the similarity is aliased. When we used 6 s windows lagged at 0.5 s the number of detections was approximately 50% of the number of detections when we used 8 s windows. When we used 9 s windows the number of detections in all four areas decreased, and decreased even more for 10 s windows to approximately 30%. When we keep the window length constant at 8 s and vary the lag at 0.25 s and 1 s, the number of detections decreased to 55% to 75% and 0% to 30%, respectively, in all four regions. Although 8 s windows lagged at 0.5 s is ideal for the time periods we analyzed in this paper, we recognize that other tremor-like activity outside of the periods we analyzed could be occurring along the Alaska-Aleutian subduction zone and these parameters would more than likely change.

[17] Following *Brown et al.* [2008], we consider a network of  $N$  channels recording ground motion in time windows represented by the vector  $u$  at time  $t_i$ . The corresponding network array autocorrelation coefficient ( $CC$ ) sum,  $A_{ij}$  is written as a correlation of the time-series with itself

$$A_{ij} = \sum_N CC_{ij}^N = u(t_i) \cdot u(t_j) \quad (1)$$

i.e., the sum of the normalized  $CC$  across the network. Summing across the network allows us to search for times when the entire network exhibits waveform similarity during tremor, and greatly enhances the ability to distinguish signal from noise and other unwanted signals. We detect on the statistics of  $A_{ij}$  relative to that of all other lags and use the median absolute deviation (MAD) to set a detection threshold [*Shelly et al.*, 2007a]. The MAD ensures that the detection statistics are not adversely affected by the fraction of the population with high values corresponding to positive detections. Pairs of time lags showing strong similarity in the autocorrelation correspond either to repeats, or near-repeats, of any signal including LFEs within the tremor. We save all window pairs that exceed our detection threshold of seven times the MAD, and define these as candidate events. We find no LFEs from autocorrelation in the times of the data where the AVO finds no tremor-like signals (Figure 5). Table 1 catalogs the regions along the arc of where and when tremor occurs. Examples of detections of repeating LFEs within continuous data are shown in Figure 5 for all four regions.

[18] Like ordinary earthquakes, LFEs from tremor in other circum-Pacific subduction zones cluster in both space and time. Closely spaced events with similar source processes should yield similar waveforms at a common station due to the similar source mechanisms and nearly identical source-receiver paths. After detecting the LFEs, we apply waveform cross-correlation for all pairs of candidate events recorded at a common station to find  $P$ - and  $S$ -wave arrivals. Next, we cross-correlate the windows at a sampling frequency of 50 Hz within a 24 s segment (appending  $\pm 8$  s to the initial window in an attempt to detect  $P$  waves). Due to the weak nature of tremor signals in general,  $P$ -waves prove to be difficult to detect; however, we are able to capture  $S$ -waves (Figure 6). We sum the waveform cross-correlation coefficients for all components across the network and save event

pairs with  $CC$  sum exceeding  $N * 0.3$ , where  $N$  = total channels used. LFE waveform alignments from the cross-correlation derived differential times are shown in Figure 7. An average coefficient value of 0.3 per component is consistent with typical  $CC$  measurements for previously detected LFEs [*Shelly et al.*, 2007a; *Brown et al.*, 2009].

#### 4. Low-Frequency Earthquake Locations

[19] We use the program *hypoDD* to estimate event locations assuming a fixed velocity model from the Alaska Earthquake Information Center (AEIC) [*Hauksson*, 1985; *Ruppert et al.*, 2011] using relative  $S$  arrival time measurements. We automate the measurement of  $S$ -wave arrival times by first choosing the peak amplitude of the absolute value of cross-correlation window pairs on all components. Next, we search for  $P$ -wave arrivals by cross-correlating 8 s window segments prior to the  $S$ -wave pick on all channels and choose the peak amplitude within the modified window with the requirement that a pick is more than 2 s behind the  $S$  arrival. This requirement ensures that any emergent  $S$  arrivals are not mispicked as  $P$  waves. Unfortunately, we are unable to identify a set of repeating  $P$  waves that are coherent across an entire network. This poses a challenge for determining an initial starting location.

[20] The *hypoDD* code can determine hypocenter locations from differenced arrival times measured by cross-correlation given a starting location for all events. We treat each tremor episode as individual event clusters. In other words, differential data is not linked from one episode to another. This criterion is important and is discussed later in this section. Since the starting locations for LFEs are unknown, we assumed 45 different candidate starting locations (see Table S1 in the supporting information) assuming all events are initially located at an assumed centroid in a grid within the four regions we find tremor-like signals.

[21] Since we know the locations of the stations recording the tremor-like signals in each region, we chose a location  $\sim 50$  km trenchward of the centroid of the stations as the spatial center of the grid, which happens to be where we would expect LFEs from tremor based on tremor/LFE epicenters in other circum-Pacific subduction zones [*Brown et al.*, 2009]. Since we do not want to rule out the possibility of events occurring in other portions of the subduction zone, we added grid nodes in both directions along strike, and in both directions inboard and outboard bringing the total number of spatial grid nodes to nine. Five depths of the grid nodes are chosen to span starting locations well above, in the vicinity of, and well below the plate interface bringing the total number of grid nodes to 45. Since the precise depth of the plate interface is not well constrained, we consider the vicinity of the plate interface to be the dipping structure illuminated by local earthquake hypocenters.

[22] We find this approach to be reasonable given the relatively small dimension of each region along the Alaska-Aleutian Arc. We use the LSQR option of *hypoDD* to iteratively minimize the residuals between observed and calculated travel-time differences and assess the quality of each starting location with respect to final locations. Despite differing starting locations for each run in each region, *hypoDD* returned a common solution (with differences in depth of less than 5 km) and where the errors of the LFE

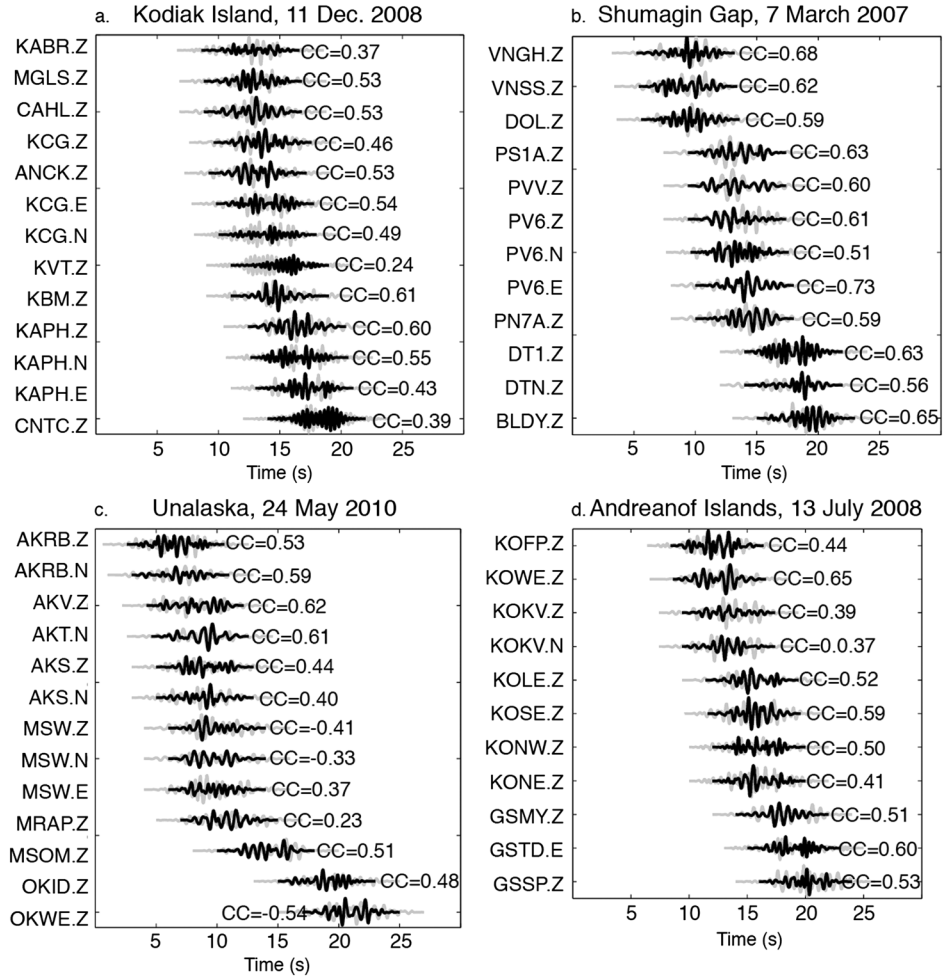


**Figure 6.** Waveform cross-correlation and moveout. Eight-second stacked windows of LFEs at a common station at (a) Kodiak Island, (b) the Shumagin Gap, (c) Unalaska, and (d) Andreanof Islands. LFE waveforms in continuous data are shown in the background in gray. Correlation coefficients of the continuous data versus the stack are shown to the right of the data.

hypocenters matched those of double-differenced local earthquake relocations [Ruppert *et al.*, 2011], so our results are not sensitive to the assumed starting location. This also verifies that the differential times from cross-correlation are  $S$  waves, consistent with observation that the majority of the energy of LFEs from tremor are from  $S$  waves [Shelly, *et al.*, 2006]. Because we have different clusters of events with 45 starting locations, we can interpret variation of starting locations in the final solution for each cluster (tremor episode) of events. We interpret the quality of all starting locations based on the maximum shift of each cluster and we consider the starting location with the smallest shift as the best starting location.

[23] There are several factors that contribute to uncertainty in the event locations. The first arises from  $S$ -wave arrival time measurements. The second source of error is from the uncertainty in the velocity structure. The errors reported for the hypocentral parameters are almost certainly underestimates [Waldhauser and Ellsworth, 2000]. Another source of uncertainty is the lack of quality  $P$ -wave arrivals. It is also worth noting that the station geometry is the biggest factor in addition to the aforementioned making relatively large uncertainties in LFE locations inevitable. Despite these

limitations we find that our approach is adequate to identify and characterize deep LFEs within tectonic tremor.

[24] We identify LFE swarms within tremor in four main regions between 2005 and 2010: Kodiak Island, the Alaska Peninsula near the Shumagin Gap, the East Aleutian Islands near Unalaska, and the Andreanof Islands near the towns of Adak and Atka.

#### 4.1. Kodiak Island

[25] We detect 156 LFEs within the six 20 min tremor episodes listed in Table 1 in the vicinity of Kodiak Island using data from a combination of stations operated by the AEIC operated by the University of Alaska at Fairbanks and the Katmai Volcanic Field operated by the AVO. To estimate LFE locations, we used 72,628  $S$ -wave cross-correlation derived differential times as input to the *hypoDD* algorithm with the AEIC velocity model used to locate earthquakes. The locations converge to approximately the same solutions indicating that our results are not sensitive to the initial locations.

[26] LFE epicenters in this area are concentrated on the north shore of Kodiak Island (Figure 8) at depths between 45 and 60 km. These events occur during January 2007,

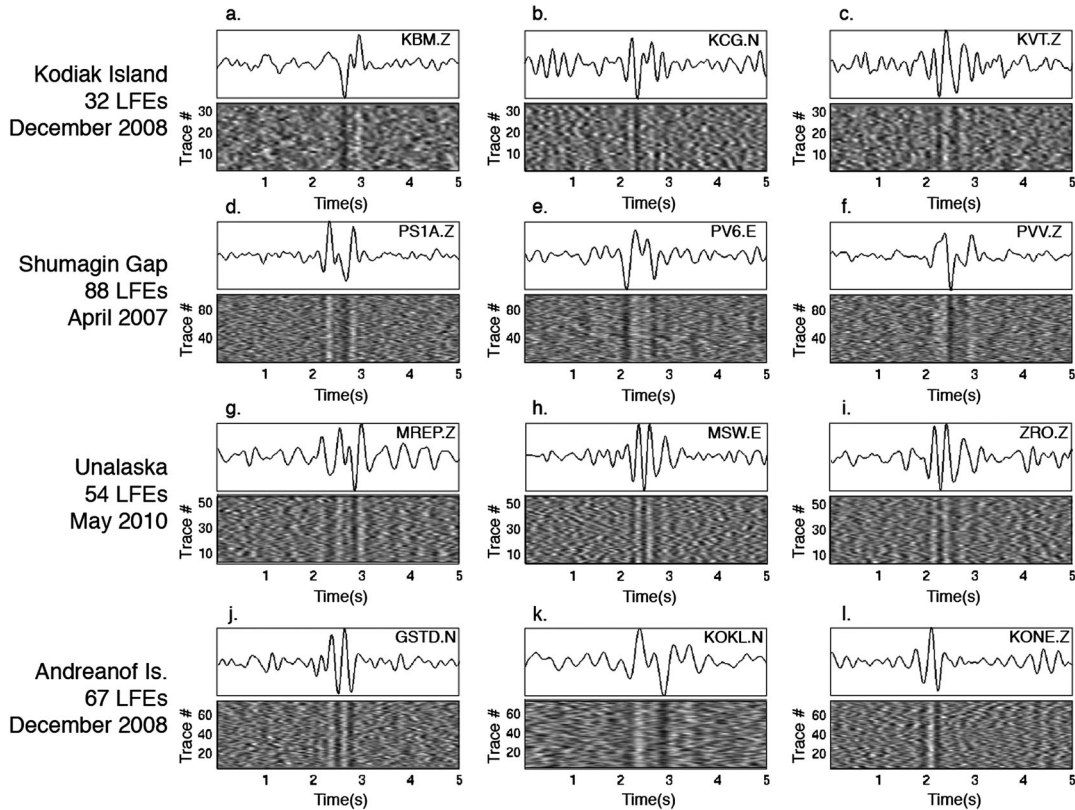


**Figure 7.** Waveform alignments and stacks. Five-second traces are plotted and aligned on the  $S$ -wave pick from cross-correlation and shown in grayscale (black =  $-1$  and white =  $+1$  amplitude) to demonstrate the detection of the  $S$ -phase arrival. Top traces show the corresponding stack.

May 2008, and December 2008 (Table S2). In cross-section the locations form a cloud of seismicity that encompasses estimates of the subducting plate interface in this region from geodetic studies and elastic dislocation models [Zweck *et al.*, 2002]. The locations of these LFEs are concentrated at the best estimate of the down-dip edge of the 1964  $M_w$  9.2 earthquake. This is consistent with hypothesis that tremor and slow slip reflect persistent frictional differences along the dip direction of the plate interface. This region includes the shallowest LFEs we report in this study.

#### 4.2. Shumagin Gap

[27] We detect 151 LFEs during two bursts of tremor activity in vicinity of the Shumagin Islands (Table 1) using data operated by the AVO. Using the same techniques and assumptions for Kodiak Island, we estimated locations using 141,090  $S$ -wave cross-correlation derived differential times.

[28] LFE epicenters in this area are concentrated on the south shore of the peninsula at depths between 50 and 60 km (Figure 9) and occur during April 2007 and March 2010 (Table S3). The locations with depth form two clouds of seismicity that encompass the best estimate of the subducting plate interface in this region. The two groups are also located in areas where the degree of coupling from east to west significantly decreases along strike. The east group of LFEs is concentrated at the best estimate of the west down-dip edge of the 1938  $M_w$  8.0 earthquake, although this location is highly uncertain. Up-dip of the LFEs, the degree of coupling on the plate interface is around 30% [Fournier

and Freymueller, 2007] and is located east of the 1993  $M_s$  6.9 earthquake [Abers *et al.*, 1995]. The west cloud is located in a patch of the Alaska-Aleutian Arc that has not ruptured in a  $M_w$  7.0+ earthquake in the last 150 yr referred to as the Shumagin Gap, where the degree of coupling is close to 0%. Geodetic measurements show the plate interface to be freely sliding [Freymueller *et al.*, 2008]. Although the possible role of tremor activity with respect to the seismic gap is uncertain, it motivates future investigations to understand the nature of deformation in this area.

#### 4.3. Unalaska

[29] We detect 278 LFEs in the vicinity of East Aleutians during eight 20 min tremor episodes (Table 1) using data from a combination of stations on Umnak, Unalaska, and Akutan Islands operated by AVO. These stations are primarily used to monitor volcanic activity at Okmok, Makushin, and Akutan volcanoes. The volcanoes in this area of the arc have recently been the most seismically active including one eruption at Okmok Caldera in 2008. We used 196,156  $S$ -wave cross-correlation derived differential times to locate the LFEs.

[30] LFE epicenters in this area are concentrated trenchward of the arc at depths between 50 and 65 km. The tremor in this area occurs during May 2007, September 2008, November 2008, February 2009, and May 2010 (Table S4). The locations with depth form some of the sharpest lineations of seismicity compared to Kodiak Island and the Shumagin Gap and are concentrated at the best estimate of the down-

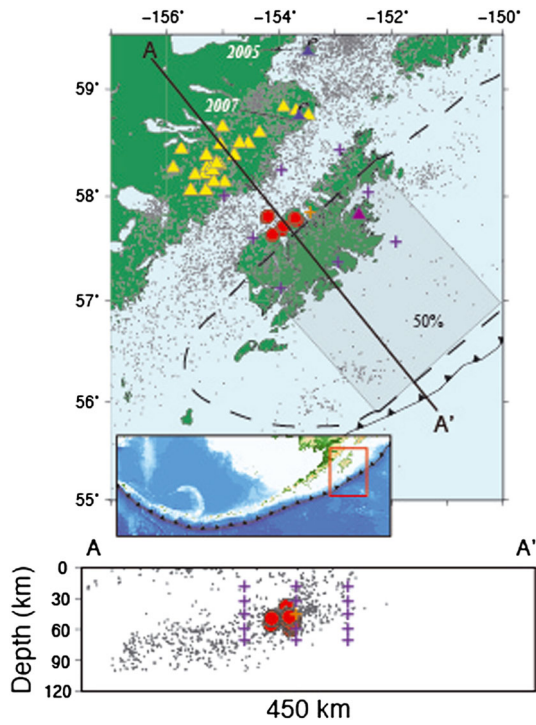


**Figure 8.** Map view and cross-sections of low-frequency earthquakes from tremor on Kodiak Island. LFEs are shown in red. Yellow triangles are stations operated by the AVO. The purple triangle is a station operated by the AEIC. Gray dots are earthquake hypocenters of  $M_w$  4 and higher from 2005–2010. The black box denotes the Kodiak asperity, which ruptured during the 1964  $M_w$  9.2 earthquake [Christensen and Beck, 1994] and the black hashed line marks the rupture patch. The estimate of plate interface coupling up-dip of the LFEs is 50% [Zweck et al., 2002]. Active volcanoes during the study are shown as violet volcano symbols. Violet crosses are the starting locations for *hypoDD*, the amber cross is the best starting location.

dip edge of the 1957  $M_w$  8.6 earthquake. Although the depths are greater, this is consistent with models of tremor and slow slip representing frictional differences along the dip direction of the plate interface. Tremor activity is the most frequent in this part of the arc.

[31] The degree of plate interface coupling trench-ward of the LFE hypocenters in this region is complex both in the along-strike and along-dip directions [Cross and Freymueller, 2008]. Plate interface coupling decreases from  $\sim 46\%$  up-dip down to  $\sim 12\%$  at the down-dip extent of the seismogenic zone in the vicinity of the two westernmost streaks of LFEs (Figure 10). For the remaining three streaks, the degree of coupling at the down-dip extent remains  $\sim 12\%$  whereas the up-dip extent decreases to 0% as it approaches the Shumagin Gap region further northeast along the strike of the subduction zone [Cross and Freymueller, 2008]. Despite these changes along strike and dip, tremor appears to span a range of coupling behaviors in this region.

#### 4.4. Andreanof Islands

[32] We detect 175 LFEs during two tremor episodes in the Central Aleutians (Table 1) using seismic stations operated by AVO. These stations are primarily used to monitor

volcanic activity at Gareloi, Tanaga, Kanaga, and Great Sitkin volcanoes (Figure 11). This area of the arc is the most remote of the U.S. Aleutian Islands considered in our study. We used 246,714 *S*-wave cross-correlation derived differential times to locate the LFEs.

[33] LFEs in this region are concentrated in two regions trench-ward of the arc. The westernmost concentration of LFEs throughout the subduction zone is on Adak Island (Figure 11) during July 2007 (Table S5). The LFEs cluster with background seismicity between 60 and 75 km depth, down-dip of the rupture extent of the 1957  $M_w$  8.6 earthquake. The second area of LFE is located on Atka Island  $\sim 120$  km east of Adak and occurred during July 2008 (Table S5). LFEs are also clustered with background seismicity between 55 and 70 km depth down-dip of the 1957 rupture. Our locations indicate this portion of the Aleutians is host to the deepest known global observations of tremor.

[34] Like Unalaska, the degree of plate interface coupling in the Andreanof Islands region is complex along strike and dip in addition to experiencing oblique subduction (Figure 1). The western cluster of LFE activity is down-dip

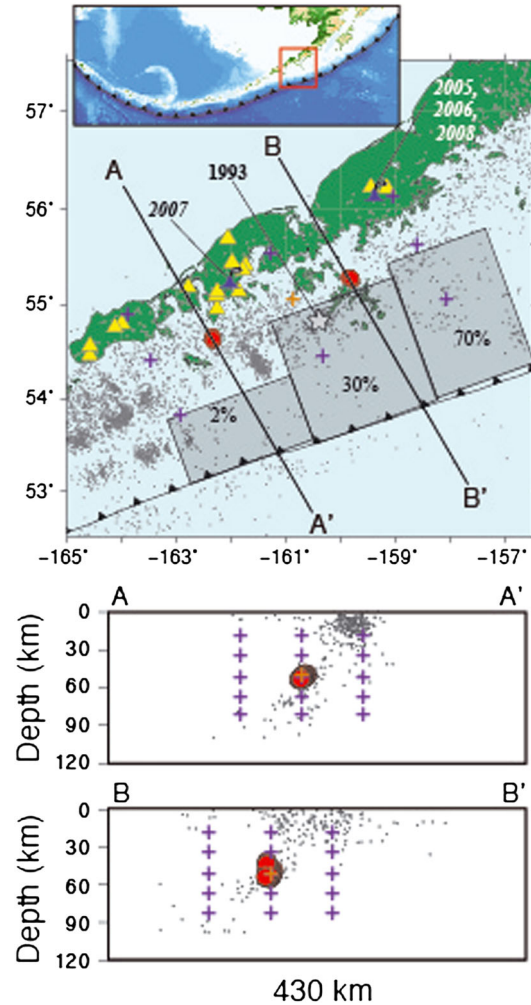


**Figure 9.** Map view and cross-sections of low-frequency earthquakes from tremor at the Shumagin Gap. Symbols are the same as in Figure 8. Variability in the degree of plate interface coupling is shown in the black boxes [Fournier and Freymueller, 2007].

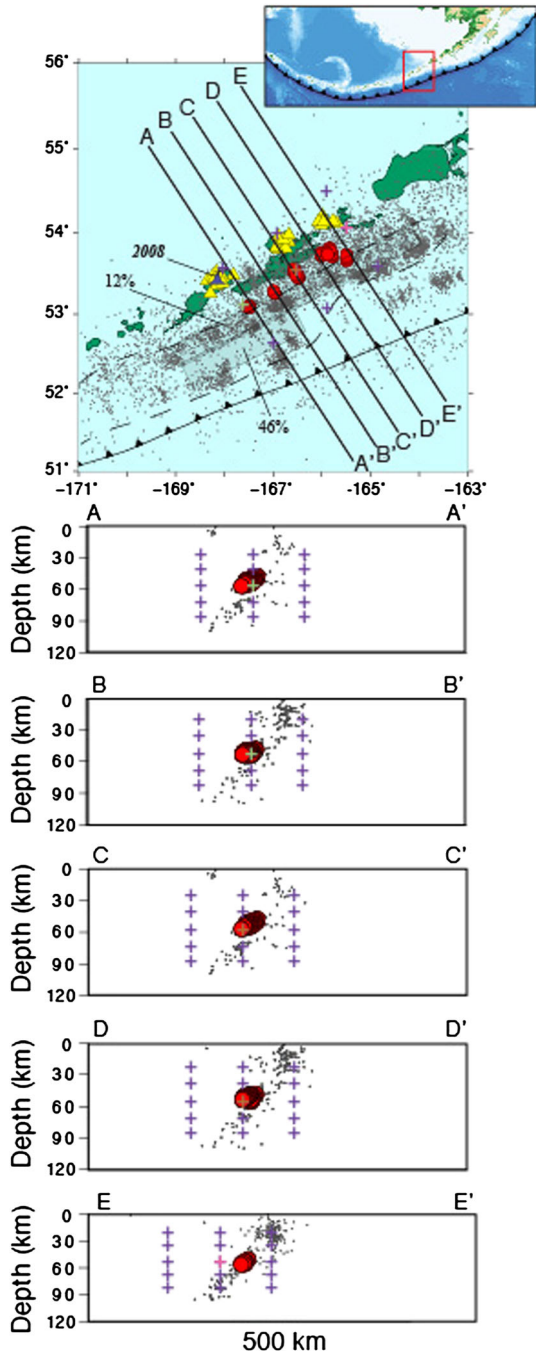


**Figure 10.** Map view and cross-sections of low-frequency earthquakes from tremor near Unalaska. Symbols are the same as in Figure 8 with the addition of the sea green and pink starting locations for clusters in their respective cross-sections. The black dashed line is an estimate of the rupture patch for the 1957  $M_w$  8.6 earthquake. Variability in the degree of plate interface coupling is shown in the black boxes [Cross and Freymueller, 2008].

from a region where the degree of coupling ranges from 13% near the trench, to fully coupled between  $\sim 20$  and  $\sim 50$  km depth. The LFEs are located down-dip of both the 1986  $M$  8.0 and 1996  $M$  7.9 rupture patches and roughly halfway between the centroid of each event (Figure 11). The degree of coupling near the eastern cluster is reversed compared

to the western cluster. The degree of coupling for the up-dip limit closest to the trench is  $\sim 79\%$  locked whereas the degree of coupling decreases to 0–25% at intermediate depths [Cross and Freymueller, 2008]. As in Unalaska, tremor activity continues to occur despite the variability of the degree of coupling along both strike and dip directions of the plate interface.

[35] To gain a better understanding of location errors, we relocated the LFEs while resampling the station geometry in the Andreanof Islands region for the westernmost cloud of LFEs detected in July 2007 (Figure 11). Figure 12 shows the spread in hypocenter locations in map view and cross-section that results. We use the centroid of the cloud as the starting epicenter and vary the starting depths at 55, 70, and 85 km. The variation in location of two LFEs is

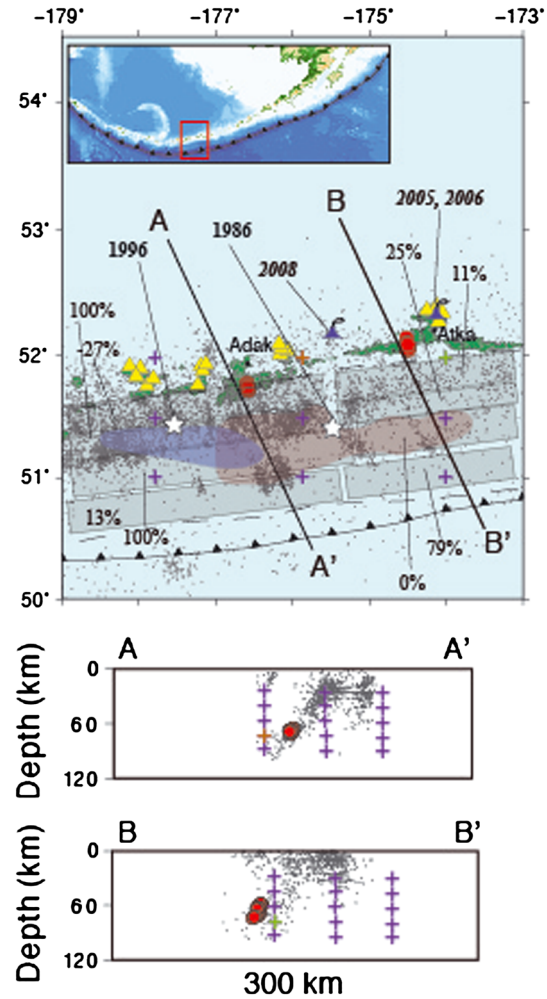


**Figure 11.** Map view and cross-sections of low-frequency earthquakes from tremor in the Andreanof Islands. Symbols are the same as in Figure 8 in addition to the sea-green cross as the best starting location for its respective cluster as shown in the cross-section. Variability in the degree of plate interface coupling is shown in the black boxes [Cross and Freymueller, 2008]. Active volcanoes during the study are shown as violet volcano symbols. The dark blue and red shaded regions correspond to the 1986  $M$  8.0 and 1996  $M$  7.9 earthquake rupture patches, respectively, with the white stars referring to their centroid.

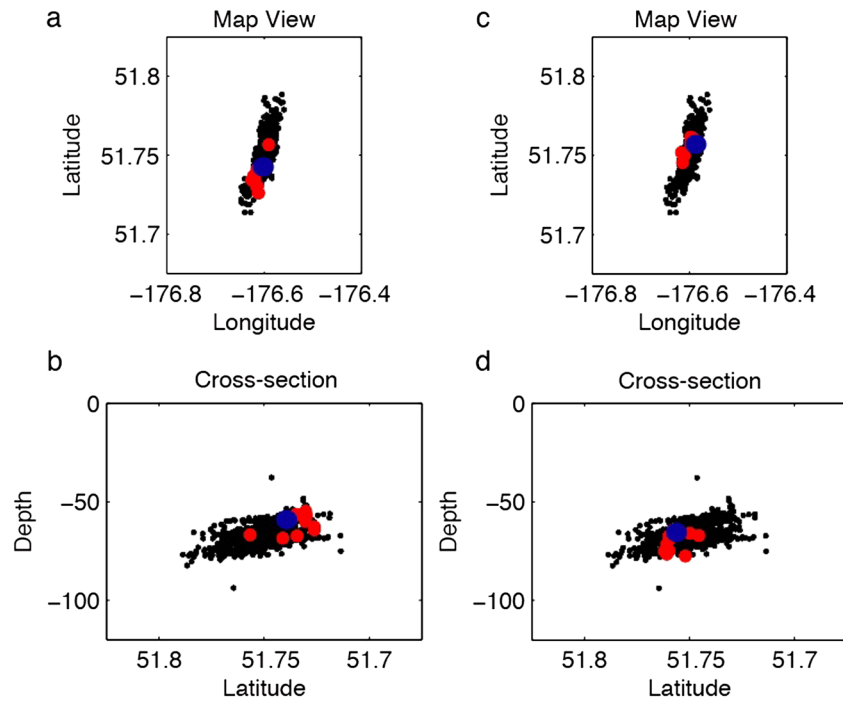


**Figure 12.** LFE locations from four different station geometries and three different starting locations for a total of 12 realizations. (a) Map view. Blue event occurred on 25 July 2007. The red events are the locations of the reference LFE for all 12 realizations. (b) Same as Figure 12a, but in cross-section. (c) Same as Figure 12a for another reference event. (d) Same as Figure 12b for a different reference event.

shown in Figures 12a, 12b and Figures 12c, 12d, respectively. The location of the centroid of LFE hypocenters is  $-176.61$  degrees longitude ( $\pm 3.5$  km),  $51.75$  degrees latitude ( $\pm 1.6$  km), and  $66.9 \pm 11.1$  km. The average 95% confidence intervals for subsets of LFEs are  $\pm 2.2$  km,  $\pm 2.4$  km, and  $\pm 12.1$  km in the longitude, latitude, and depth directions respectively.

## 5. Discussion

[36] We use the running autocorrelation of continuous waveform records from the AVO and AEIC to show that tremor-like signals in various locations along the Alaska-Aleutian Arc are composed of repeating low-frequency earthquakes. Although the locations of the events contain up to  $\pm 20$  km uncertainty in depth, the centroid of the depth distribution is within 5 km of the subducting plate interface.

[37] Tremor occurs along all parts of the Alaska-Aleutian subduction zone. It occurs along the continental part, and it occurs along the oceanic part. It occurs where there is a broad forearc high at the east end, and it occurs where there is no forearc high at the west end. It occurs where there is relatively orthogonal subduction at the east end, and it occurs where there is highly oblique subduction at the western end. Moreover, it occurs beneath Kodiak, where there is more than 1 km of late Quaternary and Holocene sediment of the Surveyor Fan entering the trench [Stevenson and Embley, 1987; von Huene et al., 2012], and it occurs beneath the Andreanof Islands where there is as little as 200 m of sediment entering the trench. Lastly, the Kodiak-Bowie seamount chain was subducted beneath Kodiak

Island [e.g., von Huene et al., 2012], and these subducted seamounts likely are in the region of the Kodiak tremor observations. No such subducted plate topography lies in the other regions where we located tremor. Thus, there are no particular characteristics of the down-going plate or overlying sediment that appear correlated with the presence or absence of tremor.

[38] In addition, there is no correlation between the presence or absence of LFEs with the degree of coupling up-dip along the megathrust. Plate interface coupling up-dip of regions of observed LFEs ranges between 2% and 100% (see Figures 8–11); therefore, the behavior of the megathrust is no predictor for the presence or absence of LFEs. This implies that the LFEs and the down-dip extent of megathrust earthquakes could be influenced by other factors such as pressure and temperature conditions.

[39] Epicenters of the LFEs are located near the down-dip extent of slip, to the extent that we know it, for previous  $M_w$  8.0+ earthquakes along the arc. This is consistent with the hypothesis that it marks a persistent difference in frictional characteristics of the subducting plate interface. The LFE locations in the Shumagin Gap could mark the down-dip extent of a future large megathrust event in that area, although understanding strain accumulation and seismic potential at the Shumagin Gap will require further study. Our LFE locations from tremor could be used to help reduce nonuniqueness in modeling the geodetic observations in this area.

[40] The age of the incoming plate interface increases across the study area from east to west, as does the incoming plate rate. The depths of the LFE activity also deepen from 45 km in the east to as deep as  $\sim 75$  km in the Andreanof

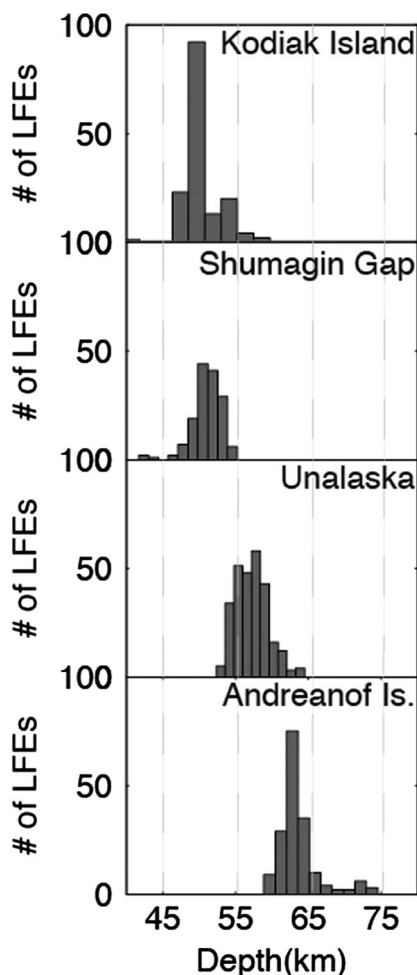


**Figure 13.** Depth distribution of tremor throughout the Alaska-Aleutian subduction zone. Depth distributions increase systematically from east to west.

Islands (Figure 13). We suspect this is due to temperature-depth variation along the arc that controls the depths to which hydrous minerals release fluids [Katsumata and Kamaya, 2003] to enable tremor activity. This will occur at greater depths when the incoming plate is older, faster, and colder.

[41] Observations of tremor in Japan strongly suggest that, where tremor occurs, it outlines the depth extent of extensive slip in large megathrust earthquakes [Ide et al., 2007]. If this holds true for Cascadia, it places rupture in large earthquakes considerably closer to the major metropolitan areas of Portland and Seattle than has been assumed previously [Chapman and Melbourne, 2009]. Our results for LFE locations near Kodiak Island suggest that tremor occurs near the down-dip extent of the 1964 Alaska earthquake, which suggests that the relationship holds there as well. Farther to the west, along the Aleutian Arc, our LFE locations are more uncertain, and it is possible that there is a gap between LFEs and large earthquake rupture zones, but that gap is small, with a depth difference of perhaps 15–20 km. Given the various degrees of coupling along strike of the Alaska-Aleutian subduction zone it is worth mentioning that a more complex model than a temperature-controlled transition between

the locking zone and tremor/LFE locations is possible [Holtkamp and Brudzinski, 2010]. More detailed studies of tremor in this area, perhaps aided by ocean bottom seismometer deployments, and of tremor in areas that have well-constrained slip distributions for large earthquake rupture, should provide a clearer picture of the relationship between tremor activity, and slip in large earthquakes.

[42] **Acknowledgments.** We thank Robert Clapp, Natalia Ruppert, Doug Christensen, and Chloe Peterson for helpful discussion. Steven McNutt, Scott Stihler, Jim Dixon, and many duty seismologists at the AVO provided a thorough daily catalog of tremor-like signals. We also thank the associate editor and two anonymous reviewers for thorough comments. J. R. B. was supported by USGS Earthquake Hazards Program and Alaska Science Center. This work was supported by NSF grant EAR-07 10835. This work utilized the Stanford Center for Computational Earth and Environmental Sciences.

## References

- Abers, G., J. Beavan, S. Horton, S. Jaumeand, and E. Triep (1995), Large accelerations and tectonic setting of the May 1993 Shumagin Islands earthquake sequence, *Bull. Seismol. Soc. Am.*, *85*, 1730–1738.
- Beroza, G. C., and S. Ide (2011), Slow earthquakes and nonvolcanic tremor, *Annual Rev. Planet. Earth Sci.*, *39*, pp. 271–296.
- Brown, J. R., G. C. Beroza, and D. R. Shelly (2008), An autocorrelation-method to detect low frequency earthquakes within tremor, *Geophys. Res. Lett.*, *35*, L16305, doi:10.1029/2008GL034560.
- Brown, J. R., G. C. Beroza, S. Ide, K. Ohta, D. R. Shelly, S. Y. Schwartz, W. Rabbel, M. Thorwart, and H. Kao (2009), Deep low-frequency earthquakes in tremor localize to the plate interface in multiple subduction zones, *Geophys. Res. Lett.*, *36*, L19306, doi:10.1029/2009GL040002.
- Cervelli, D. P., P. Cervelli, A. Miklius, R. Krug, and M. Lisowski (2002), VALVE: Volcano Analysis and Visualization Environment, American Geophysical Union, Fall Meeting 2002, abstract #U52A-07.
- Chapman, J. S., and T. I. Melbourne (2009), Future Cascadia megathrust rupture delineated by episodic tremor and slip, *Geophys. Res. Lett.*, *36*, doi:10.1029/2009GL040465.
- Chouet, B. (1985), Excitation of a buried magmatic pipe: a seismic source model for vol- canic tremor. *J. Geophys. Res.*, *90*, 1881–1893.
- Christensen, D. H., and S. L. Beck (1994), The rupture process and implications of the great 1964 Prince William Sound earthquake, *Pure and Applied Geophys.*, doi:10.1007/BF00875967
- Cross, R. S., and J. T. Freymueller (2008), Evidence for implications of a Bering plate based on geodetic measurements from the Aleutians and western Alaska, *J. Geophys. Res.*, *113*, B07405, doi:10.1029/2007JB005136.
- DeMets, C., R. G. Gordon, D. F. Argus and S. Stein (1994), Effect of recent revisions to the geomagnetic reversal timescale, *Geophys. Res. Lett.*, *21*, 2191–2194.
- Fournier, T. J., and J. T. Freymueller (2007), Transition from locked to creeping subduction in the Shumagin region, Alaska, *Geophys. Res. Lett.*, *34*, L06303, doi:10.1029/2006GL029073.
- Freymueller, J. T., H. Woodard, S. Cohen, R. Cross, J. Elliott, C. Larsen, S. Hreinsdottir, and C. Zweck (2008), Active deformation processes in Alaska, based on 15 years of GPS measurements, in *Active Tectonics and Seismic Potential of Alaska*, AGU Geophysical Monograph, 179, J. T. Freymueller, P. J. Haeussler, R. Wesson and G. Ekstrom, eds., pp. 1–42, AGU, Washington, D.C.
- Gomberg, J. S. (2010), Introduction of a special section on Phenomenology, Underlying Processes, and Hazard Implications of Aseismic Slip and nonvolcanic tremor, *J. Geophys. Res.*, *115*, B00A00, doi:10.1029/2010JB008052.
- Hauksson, E. (1985), Structure of the Benioff zone beneath the Shumagin Islands, Alaska: relocation of local earthquakes using three-dimensional ray tracing, *J. Geophys. Res.*, (90), pp. 635–649.
- Hauksson, E., J. Armbruster, and S. Dobbs (1984), Seismicity patterns (1963–1983) as stress indicators in the Shumagin seismic gap, Alaska, *Bull. Seismol Soc Amer.*, *74*, pp 2541–2558.
- Hellweg, M. (2000), Physical models for the source of Lascar’s harmonic tremor, *J. Volc. and Geothermal Res.*, *101*, 183–198
- Holtkamp, S., and M. R. Brudzinski (2010), Determination of slow slip episodes and strain accumulation along the Cascadia margin, *J. Geophys. Res.*, *115*, B00A17, doi:10.29/2008JB006058.
- Ide, S., D. R. Shelly, and G. C. Beroza (2007), The mechanism of deep low frequency earthquakes: further evidence that deep non-volcanic tremor is generated by shear slip on the plate interface, *Geophys. Res. Lett.*, *34*, L03308, doi:10.1029/2006GL028890.

- Johnson, J. B., and J. M. Lees (2000), Plugs and chugs—seismic and acoustic observations of degassing explosions at Karymsky, Russia and Sangay, Ecuador. *J. Volc. Geothermal Res.* **101**, 67–82.
- Julian, B. R. (1994), Volcanic tremor: nonlinear excitation by fluid flow, *J. Geophys. Res.*, **99**, 11859–11877.
- Kao, H., P. J. Thompson, G. Rogers, H. Dragert, and G. Spence (2007), Automatic detection and characterization of seismic tremors in northern Cascadia. *Geophys. Res. Lett.*, **34**, L16313, doi:10.1029/2007GL030822.
- Kao, H., P. J. Thompson, S.-J. Shan, G. Rogers, and H. Dragert (2008), Tremor Activity Monitoring in Northern Cascadia, *Eos Trans. AGU*, **89**(42), 405, doi:10.1029/2008EO420001.
- Katsumata, A., and N. Kamaya (2003), Low-frequency continuous tremor around the Moho discontinuity away from volcanoes in the southwest Japan, *Geophys. Res. Lett.*, **30**(1), 1020, doi:10.1029/2002GL015981.
- McNutt, S. R. (1992), Volcanic tremor, Encyclopedia of earth system science, vol 4, Academic Press, San Diego, pp. 417–425.
- Obara, K. (2002), Nonvolcanic deep tremor association with subduction in southwest Japan, *Science*, **296**, pp. 1679–1681.
- Ohta, Y., J. T. Freymueller, S. Hreinsdottir, and H. Suito (2006), A large slow slip event and the depth of seismogenic zone in the south central Alaska subduction zone, *Earth and Planet. Sci. Lett.*, **247**, pp. 108–116.
- Peterson, C. L., S. R. McNutt, and D. H. Christensen (2011), Nonvolcanic tremor in the Aleutian Arc, *Bull. Seismo. Soc. Amer.*, **101**, pp. 3081–3087.
- Rogers, G., and H. Dragert (2003), Episodic tremor and slip in Cascadia subduction zone: The chatter of silent slip, *Science*, **300**, pp. 1942–1943.
- Rubinstein J. L., D. R. Shelly, and W. L. Ellsworth (2010), Non-volcanic tremor: A window into the roots of fault zones, in *New Frontiers of Solid Earth Sciences*, doi:10.1007/987-90-481-2737-5 8.
- Ruppert, N. A., J. M. Lees, and N. P. Kozyreva (2007), Seismicity, earthquakes and rupture along the Alaska-Aleutian and Kamchatka-Kurile subduction zones: a review, *Volcanism and Subduction*, Geophys. Monograph **172**.
- Ruppert, N. A., N. P. Kozyreva, and R. A. Hansen (2011), Review of crustal seismicity in the Aleutian Arc and implications for arc deformation, *Tectonophysics*, doi:10.1016/j.tecto.2011.03.031.
- Schwartz, S. Y., and J. M. Rokosky (2007), Slow slip events and seismic tremor and circum-Pacific subduction zones, *Rev. Geophys.*, **45**, pp. 1–32.
- Shelly, D. R., G. C. Beroza, S. Ide, and S. Nakamura (2006), Low-frequency earthquakes in Shikoku, Japan, and their relationship to episodic tremor and slip, *Nature*, **442**, 188–191, doi:10.1038/nature04931.
- Shelly, D. R., G. C. Beroza, and S. Ide (2007a), Non-Volcanic Tremor and Low Frequency Earthquake Swarms, *Nature* **446**, 305–307, doi:10.1038/nature05666.
- Shelly, D. R., G. C. Beroza, and S. Ide (2007b), Complex evolution of transient slip derived from precise tremor locations in western Shikoku, Japan, *Geochem. Geophys. Geosyst.*, **8**, Q10014, doi:10.1029/2007GC001640.
- Stevenson, A. J., and Embley, R. (1987), Deep Sea Fan Bodies, Terrigenous Turbidite Sedimentation, and Petroleum Geology, Gulf of Alaska, in Scholl, D. W., A. Grantz, and J. G. Vedder, eds., *Geology and resource, Potential of the continental margin of western N. America and adjacent ocean basins - Beaufort Sea to Baja California: American Association-Petroleum*, *Geology*, p. 503–522.
- Von Huene, R., J. J. Miller, and W. Weinrebe (2012), Subducting plate geology in three great earthquake ruptures of the western Alaska margin, *Kodiak to Umnak: Geosphere*, doi:10.1130/GES00715.1.
- Waldhauser, F., and W. L. Ellsworth (2000), A double-difference earthquake location algorithm: Method and application to the northern Hayward fault, California, *Bull. Seismol. Soc. Am.*, **6**, 1353–136.
- Wech, A. G., and K. C. Creager (2008), Automated detection and location of Cascadia tremor, *Geophys. Res. Lett.*, **35**, L20302, doi:10.1029/2008GL03545.
- Zweck, C., J. T. Freymueller, and S. C. Cohen (2002), Three-dimensional elastic dislocation modeling of the postseismic response to the 1964 Alaska earthquake, *J. Geophys. Res.*, vol. **107**, (B4), 2064, doi:10.1029/2001JB000409./2001JB000409.